

Manuscript gmd-2014-198

Original Title: *Simulation of groundwater and surface water over the continental US using a hyperresolution, integrated hydrologic model.*

Current Title: *A high resolution simulation of groundwater and surface water over most of the continental US with the integrated hydrologic model ParFlow v3.*

2-Feb-15

*Dr Jeff Neal*

*Lecturer*

*Topical Editor (Hydrology) - Geoscientific Model Development*

*School of Geographical Sciences*

*University of Bristol*

Dear Jeff:

We have respectfully submitted a revised manuscript for the submission gmd-2014-198. We provided detailed replies to all three sets of comments (R1, R2 and the ED) using the online interactive system. We also provided a PDF of all the changes (highlighted in red, using word's mark-up system) from the version of the manuscript sent for typesetting on 16-Oct-14 and this current, revised version. Where possible, we have tried to connect revisions to the manuscript to the reviewer comment replies, but given the interactive process this is somewhat challenging so we would like to draw your attention to the following general areas of revision:

1. Title: as you see above, we have revised the title given the concerns regarding the use of the term 'hyperresolution'. We have also changed other language throughout the manuscript to be consistent with this change.
2. Intent. While we feel that our work is well-motivated, we have added text throughout the manuscript to further clarify our intended outcomes.
3. Uncertainty and data limitations. We have added language about data limitations and uncertainty throughout the manuscript; introduction, discussion and conclusions.
4. Typographical. We have increased font sizes on figures, fixed references etc.

We appreciate the time and effort put in by both reviewers. Reviewer 1 was very complementary and provided quite constructive comments, all of which have been reflected by revisions in the updated manuscript. We were disappointed by the unprofessional tone of Reviewer 2 and their attempts to distort our work and its intent. As you will see in our replies, many of the comments by this reviewer were not accurate: we did address uncertainty in the original manuscript ("no mention of uncertainty"), did not overstate the goodness of fit ("with fits like these what could possibly be wrong"), etc. Still, we have made every effort to both clarify our perspective and expand our discussion of limitations. Unfortunately, based on the tenor of R2's comments it is apparent that we have fundamentally different viewpoints and it seems unlikely that our responses or revisions will change their opinion regarding publication. We feel there will

be tremendous interest in this work, which has been viewed at least 239 times (downloaded at least 116 as a PDF) while under discussion. We reiterate that this is a novel contribution and that no-other comprehensive model at such high resolution over such large scales exists.

We thank you for your time and attention to this matter. We are happy to answer any additional questions you might have, and we look forward to hearing your decision on the status of this manuscript.

Sincerely,  
Reed

*Reed M. Maxwell, Ph.D.  
Professor  
Department of Geology and Geologic Engineering  
Colorado School of Mines  
1500 Illinois St.  
Golden, Co 80401*

[A high resolution simulation](#) of groundwater and surface water over [most of](#) the continental US  
[with the](#) integrated hydrologic model [ParFlow v3](#)

Reed M Maxwell<sup>1\*</sup>, Laura E Condon<sup>1</sup>, Stefan J Kollet<sup>2</sup>

<sup>1</sup>Hydrologic Science and Engineering Program, Integrated GroundWater Modeling Center, Department  
of Geology and Geological Engineering, Colorado School of Mines, Golden, Colorado, USA

<sup>2</sup>Centre for High-Performance Scientific Computing in Terrestrial Systems, Institute for Bio- and  
Geosciences, Agrosphere (IBG-3), Research Centre Jülich, Jülich, DE

\*correspondence to: Reed M Maxwell, rmaxwell@mines.edu

## Abstract

Interactions between surface and groundwater systems are well-established theoretically and  
observationally. While numerical models that solve both surface and subsurface flow equations  
in a single framework (matrix) are increasingly being applied, computational limitations have  
restricted their use to local and regional studies. Regional or watershed-scale simulations have  
been effective tools in understanding hydrologic processes, however there are still many  
questions, such as the adaptation of water resources to anthropogenic stressors and climate  
variability, that need to be answered across large spatial extents at high resolution. In response  
to this ‘grand challenge’ in hydrology, we present the results of a parallel, integrated hydrologic  
model simulating surface and subsurface flow at high spatial resolution (1km) over much of  
continental North America (~6,300,000 or 6.3M km<sup>2</sup>). These simulations provide [integrated](#)  
predictions of hydrologic states and fluxes, namely water table depth and streamflow, at [very](#)  
[large](#) scale and [high](#) resolution. The [physics](#)-based modeling approach used here requires limited  
parameterizations and relies only on more fundamental inputs, such as topography,  
hydrogeologic properties and climate forcing. Results are compared to observations and provide  
mechanistic insight into hydrologic process interaction. This study demonstrates both the  
feasibility of continental scale integrated models and their utility for improving our  
understanding of large-scale hydrologic systems; the combination of high resolution and large  
spatial extent facilitates novel analysis of scaling relationships using model outputs.

Reed Maxwell 2/2/2015 5:06 AM

Deleted: Simulation

Reed Maxwell 2/2/2015 5:06 AM

Deleted: using a hyperresolution,

Reed Maxwell 2/2/2015 5:06 AM

Deleted: ,

Reed Maxwell 2/2/2015 5:06 AM

Deleted: unprecedented

Reed Maxwell 2/2/2015 5:06 AM

Deleted: physically

## 36 Introduction

37 There is growing evidence of feedbacks between groundwater, surface water and soil  
38 moisture that moderate land-atmospheric energy exchanges, and impact weather and climate  
39 [\(Maxwell et al. 2007; Anyah et al. 2008; Kollet and Maxwell 2008; Maxwell and Kollet 2008;](#)  
40 [Jiang et al. 2009; Rihani et al. 2010; Maxwell et al. 2011; Williams and Maxwell 2011; Condon](#)  
41 [et al. 2013; Taylor et al. 2013\)](#). While local observations and remote sensing can now detect  
42 changes in the hydrologic cycle from small to very large spatial scales (e.g. Rodell et al. 2009),  
43 theoretical approaches to connect and scale hydrologic states and fluxes from point  
44 measurements to the continental scales are incomplete. In this work, we present integrated  
45 modeling as one means to bridge this gap [via numerical experiments](#).

46 Though introduced as a concept in the literature almost half a century ago (Freeze and  
47 Harlan 1969), integrated hydrologic models that solve the surface and subsurface systems  
48 simultaneously have only been a reality for about a decade (VanderKwaak and Loague 2001;  
49 Jones et al. 2006; Kollet and Maxwell 2006). Since their implementation, integrated hydrologic  
50 models have been successfully applied to a wide range of watershed-scale studies (see Table 1 in  
51 Maxwell et al. 2014) successfully capturing observed surface and subsurface behavior (Qu and  
52 Duffy 2007; Jones et al. 2008; Sudicky et al. 2008; Camporese et al. 2010; Shi et al. 2013),  
53 diagnosing stream-aquifer and land-energy interactions (Maxwell et al. 2007; Kollet and  
54 Maxwell 2008; Rihani et al. 2010; Condon et al. 2013; Camporese et al. 2014), and building our  
55 understanding of the propagation of perturbations such as land-cover and anthropogenic climate  
56 change throughout the hydrologic system (Maxwell and Kollet 2008; Goderniaux et al. 2009;  
57 Sulis et al. 2012; Mikkelsen et al. 2013).

Reed Maxwell 2/2/2015 5:06 AM

**Deleted:** (Maxwell et al. 2007;

Reed Maxwell 2/2/2015 5:06 AM

**Deleted:** ; Kollet and Maxwell 2008;  
Maxwell and Kollet 2008; Jiang et al. 2009;  
Rihani et al. 2010; Maxwell et al. 2011;  
Williams and Maxwell 2011; Condon et al.  
2013; Taylor et al. 2013)



64 Prior to this work, computational demands and data constraints have limited the  
65 application of integrated models to regional domains. Advances in parallel solution techniques,  
66 numerical solvers, supercomputer hardware, and additional data sources have only recently made  
67 large-scale, high-resolution simulation of the terrestrial hydrologic cycle technically feasible  
68 (Kollet et al. 2010; Maxwell 2013). As such, existing large scale studies of the subsurface have  
69 focused on modeling groundwater independently (Fan et al. 2007; Miguez-Macho et al. 2007;  
70 Fan et al. 2013) and classifying behavior with analytical functions (Gleeson et al. 2011).  
71 Similarly, continental scale modeling of surface water has utilized tools with simplified  
72 groundwater systems that do not capture lateral groundwater flow and model catchments as  
73 isolated systems (Maurer et al. 2002; Döll et al. 2012; Xia et al. 2012), despite the fact that lateral  
74 flow of groundwater has been shown to be important across scales (Krakauer et al. 2014). While  
75 much has been learned from previous studies, the focus on isolated components within what we  
76 know to be an interconnected hydrologic system is a limitation that can only be addressed with  
77 an integrated approach.

78 The importance of groundwater surface water interactions in governing scaling behavior  
79 of surface and subsurface flow from headwaters to the continent has yet to be fully characterized.  
80 Indeed, one of the purposes for building an integrated model is to better understand and predict  
81 the nature of hydrologic connections across scales and throughout a wide array of physical and  
82 climate settings. Arguably, this is not possible utilizing observations, because of data scarcity  
83 and the challenges observing 3D groundwater flow across a wide range of scales. For example,  
84 the scaling behavior of river networks is well known (Rodriguez-Iturbe and Rinaldo 2001), yet  
85 open questions remain about the quantity, movement, travel time, and spatial and temporal  
86 scaling of groundwater and surface water at the continental scale. Exchange processes and flow

Reed Maxwell 2/2/2015 5:06 AM

Deleted: the

Reed Maxwell 2/2/2015 5:06 AM

Deleted: . Despite

Reed Maxwell 2/2/2015 5:06 AM

Deleted: (Nir et al. 2014)

Reed Maxwell 2/2/2015 5:06 AM

Deleted: scale

91 near the land surface are strongly non-linear, and heterogeneity in hydraulic properties exist at all  
92 spatial scales. As such, a formal framework for connecting scales in hydrology (Wood 2009)  
93 needs to account for changes in surface water and groundwater flow from the headwaters to the  
94 mouth of continental river basins. We propose that integrated, physics-based hydrologic models  
95 are a tool for providing this understanding, solving fundamental non-linear flow equations at  
96 high spatial resolution while *numerically* scaling these physical processes up to a large spatial  
97 extent i.e. the continent.

98 In this study, we simulate surface and subsurface flow at high spatial resolution (1km)  
99 over much of continental North America (6.3M km<sup>2</sup>), which is itself considered a grand  
100 challenge in hydrology (e.g. Wood et al. 2011; Gleeson and Cardiff 2014). The domain is  
101 constructed entirely of available datasets including topography, soil texture and hydrogeology  
102 This simulation solves surface and subsurface flow simultaneously and takes full advantage of  
103 massively parallel, high-performance computing. The results presented here should be viewed as  
104 a sophisticated numerical experiment, designed to diagnose physical behavior and evaluate  
105 scaling relationships. While this is not a calibrated model that is intended to match observations  
106 perfectly, we do verify that behavior is realistic by comparing to both groundwater and surface  
107 water observations.

108 The paper is organized as follows: first a brief description of the model equations are  
109 provided including a description of the input variables and observational datasets used for model  
110 comparison; next model simulations are compared to observations in a number of ways, and then  
111 used to understand hydrodynamic characteristics and to describe scaling.

112  
113

Reed Maxwell 2/2/2015 5:06 AM

**Deleted:** (~6,300,000 or

Reed Maxwell 2/2/2015 5:06 AM

**Deleted:** .

Reed Maxwell 2/2/2015 5:06 AM

**Deleted:** The domain is constructed entirely of available datasets including topography, soil texture and hydrogeology. Results are compared to observations, and used

## 120 **Methods**

121 The model was constructed using the integrated simulation platform ParFlow (Ashby and  
122 Falgout 1996; [Jones and Woodward 2001](#); [Kollet and Maxwell 2006](#)) utilizing the terrain  
123 following grid capability (Maxwell 2013). ParFlow is a physically based model that solves both  
124 the surface and subsurface systems simultaneously. In the subsurface ParFlow solves the mixed  
125 form of Richards' equation for variably saturated flow (Richards 1931) in three spatial  
126 dimensions given as:

$$127 \quad S_s S_w(h) \frac{\partial h}{\partial t} + \phi S_w(h) \frac{\partial S_w(h)}{\partial t} = \nabla \cdot \mathbf{q} + q_r(x, z) \quad (1)$$

128 where the flux term  $\mathbf{q}$  [ $\text{LT}^{-1}$ ] is based on Darcy's law:

$$129 \quad \mathbf{q} = -\mathbf{K}_s(\mathbf{x}) k_r(h) [\nabla(h + z) \cos \theta_x + \sin \theta_x] \quad (2)$$

130 In these expressions,  $h$  is the pressure head [ $\text{L}$ ];  $z$  is the elevation with the  $z$ -axis specified as  
131 upward [ $\text{L}$ ];  $\mathbf{K}_s(\mathbf{x})$  is the saturated hydraulic conductivity tensor [ $\text{LT}^{-1}$ ];  $k_r$  is the relative  
132 permeability [-];  $S_s$  is the specific storage [ $\text{L}^{-1}$ ];  $\phi$  is the porosity [-];  $S_w$  is the relative saturation [-]  
133 ];  $q_r$  is a general source/sink term that represents transpiration, wells, and other fluxes [ $\text{T}^{-1}$ ]; and  
134  $\theta$  [-] is the local angle of slope, in the  $x$  and  $y$  directions and may be written as

135  $\theta_x = \tan^{-1} S_x$  and  $\theta_y = \tan^{-1} S_y$ . Note that we assume that density and viscosity are both

136 constant, [although ParFlow can simulate density and viscosity-dependent flow](#) (Kollet et al.

137 2009). The van Genuchten (1980) relationships are used to describe the relative saturation and  
138 permeability functions ( $S_w(h)$  and  $k_r(h)$  respectively). These functions are highly nonlinear and  
139 characterize changes in saturation and permeability with pressure.

140 Overland flow is represented in ParFlow by the two-dimensional kinematic wave  
141 equation resulting from application of continuity conditions for pressure and flux (Kollet and  
142 Maxwell 2006):

Reed Maxwell 2/2/2015 5:06 AM

**Deleted:** ; Jones and Woodward 2001; Kollet and Maxwell 2006)

Reed Maxwell 2/2/2015 5:06 AM

**Deleted:** though this assumption is not necessarily needed in

$$\mathbf{k} \cdot (-\mathbf{K}_s(\mathbf{x})k_r(h) \cdot \nabla(h+z)) = \frac{\partial \|h,0\|}{\partial t} - \nabla \cdot \|h,0\| \mathbf{v}_{sw} + \lambda q_r(\mathbf{x}) \quad (3)$$

In this equation  $\mathbf{v}_{sw}$  is the two-dimensional, depth-averaged surface water velocity [ $\text{LT}^{-1}$ ] given by Manning's equation;  $h$  is the surface ponding depth [L] the same  $h$  as is shown in Equation 1. Note that  $\|h,0\|$  indicates the greater value of the two quantities in Equation 3. This means that if  $h < 0$  the left hand side of this equation represents vertical fluxes (e.g. in/exfiltration) across the land surface boundary and is equal to  $q_r(\mathbf{x})$  and a general source/sink (e.g. rainfall,  $ET$ ) rate [ $\text{LT}^{-1}$ ] with  $\lambda$  being a constant equal to the [inverse of the](#) vertical grid spacing [ $\text{L}^{-1}$ ]. This term is then entirely equivalent to the source/sink term shown in Equation 1 at the ground surface where  $\mathbf{k}$  is the unit vector in the vertical, again defining positive upward coordinates. If  $h > 0$  then the terms on the right hand side of Equation 3 are active water that is routed according to surface topography (Kollet and Maxwell 2006).

The nonlinear, coupled equations of surface and subsurface flow presented above are solved in a fully-implicit manner using a parallel Newton-Krylov approach (Jones and Woodward 2001; Kollet and Maxwell 2006; Maxwell 2013). Utilizing a globally-implicit solution allows for interactions between the surface and subsurface flow system to be explicitly resolved. While this yields a very challenging computational problem, ParFlow is able to solve large complex systems by utilizing a multigrid preconditioner ([Osei-Kuffuor et al. ; Ashby and Falgout 1996](#)) and taking advantage of highly scaled parallel efficiency out to more than  $1.6 \times 10^4$  processors (Kollet et al. 2010; Maxwell 2013).

[Physically this means that ParFlow solves saturated subsurface flow \(i.e. groundwater\), unsaturated subsurface flow \(i.e. the vadose zone\) and surface flow \(i.e. streamflow\) in a continuum approach within a single matrix. Thus, complete non-linear interactions between all system components are simulated without \*a priori\* specification of what types of flow occur in](#)

Reed Maxwell 2/2/2015 5:06 AM

**Deleted:** (Osei-Kuffuor et al. ;

Reed Maxwell 2/2/2015 5:06 AM

**Deleted:** Physically this means that ParFlow solves saturated subsurface flow (i.e. groundwater), unsaturated subsurface flow (i.e. the vadose zone) and surface flow (i.e. streamflow) in a continuum approach within a single matrix. Thus, complete non-linear interactions between all system components are simulated without *a priori* specification of what types of flow occur in any given portion of the grid. Streams form purely based on hydrodynamic principles governed by recharge, topography, hydraulic conductivity and flow parameters, when water is ponded due to either excess infiltration (surface fluxes exceed the infiltration capacity) or excess saturation (subsurface exfiltration to the surface system). Groundwater converges in topographic depressions and unsaturated zones may be shallow or deep depending upon recharge and lateral flows.

191 [any given portion of the grid. Streams form purely based on hydrodynamic principles governed](#)  
192 [by recharge, topography, hydraulic conductivity and flow parameters, when water is ponded due](#)  
193 [to either excess infiltration \(surface fluxes exceed the infiltration capacity, e.g. Horton 1933\) or](#)  
194 [excess saturation \(subsurface exfiltration to the surface system, e.g. Dunne 1983\) for further](#)  
195 [discussion see Kirkby \(1988\) and Beven \(2004\) for example. Groundwater converges in](#)  
196 [topographic depressions and unsaturated zones may be shallow or deep depending upon recharge](#)  
197 [and lateral flows.](#)

198       The physically based approach used by ParFlow is similar to other integrated hydrologic  
199 models such as Hydrogeosphere (Therrien et al. 2012), PIHM (Kumar et al. 2009) and CATHY  
200 (Camporese et al. 2010). This is a distinct contrast [to](#) more conceptually-based models that may  
201 not simulate lateral groundwater flow or [simplify the solution of surface and subsurface flow by](#)  
202 [defining regions of groundwater or the stream-network prior to the simulation. In such models,](#)  
203 [groundwater surface water interactions are often captured as one-way exchanges \(i.e. surface](#)  
204 [water loss to groundwater\) or parameterized with simple relationships \(i.e. \[functional\]\(#\)](#)  
205 [relationships](#) to impose the relationship between stream head and baseflow). The integrated  
206 approach used by ParFlow eliminates the need for such assumptions and allows the  
207 interconnected groundwater surface water systems to evolve dynamically based only on the  
208 governing equations and the properties of the physical system. The approach used here requires  
209 robust numerical solvers ([Maxwell 2013; Osei-Kuffuor et al. 2014](#)) and exploits high-  
210 performance computing ([Kollet et al. 2010](#)) to achieve high resolution, large extent simulations.

211

212

213

Reed Maxwell 2/2/2015 5:06 AM

Deleted: with

Reed Maxwell 2/2/2015 5:06 AM

Deleted: may

Reed Maxwell 2/2/2015 5:06 AM

Deleted: ,

Reed Maxwell 2/2/2015 5:06 AM

Deleted: curves

## 218 Domain Setup

219 In this study, the model [and numerical experiment was directed at](#) the Continental US  
220 (CONUS) [using the terrain following grid framework \(Maxwell 2013\)](#) for a total thickness of  
221 102m over 5 model layers. The model was implemented with a lateral resolution of 1km with  
222  $n_x=3342$ ,  $n_y=1888$  and five vertical layers with 0.1, 0.3, 0.6, 1.0 and 100m discretization for a  
223 total model dimensions of 3,342 by 1,888 by 0.102 km and 31,548,480 total compute cells. The  
224 model domain and input data sets are shown in Figure 1. All model inputs were re-projected to  
225 have an equal cell-size of [1x1km](#) as shown in Figure 1. Topographic slopes ( $S_x$  and  $S_y$ ) were  
226 calculated from the Hydrosheds digital elevation model (Figure 1b) and were processed using the  
227 r.watershed package in the GRASS GIS platform. [Surface roughness values were constant  \$10^{-5}\$](#)   
228 [\[h m<sup>-1/3</sup>\] outside of the channels and varied within the channel as a function of average](#)  
229 [watershed slope.](#) Over the top 2m of the domain, hydraulic properties from soil texture  
230 information of SSURGO were applied and soil properties were obtained from Schaap and Leij  
231 (1998) . Note that two sets of soil categories were available. The upper horizon was applied over  
232 the top 1m (the top three model layers) and the bottom one over the next 1m (the fourth model  
233 layer). Figures 1a and c show the top and bottom soil layers of the model. The deeper subsurface  
234 (i.e. below 2m) was constructed from a global permeability map developed by Gleeson et al.  
235 (2011). These values (Gleeson et al. 2011) were adjusted to reduce variance (Condon and  
236 Maxwell 2013; Condon and Maxwell 2014) and to reflect changes in topography using the e-  
237 folding relationship empirically-derived in (Fan et al. 2007):  $\alpha = e^{-\frac{50}{f}}$  where  $f = \frac{a}{(1+b*\sqrt{S_x^2+S_y^2})}$   
238 . For this analysis  $a=20$ ,  $b=125$  and the value of 50 [m] was chosen to reflect the midpoint of the  
239 deeper geologic layer in the model. Larger values of  $\alpha$  reduced the hydraulic conductivity  
240 categorically, that is by decreasing the hydraulic conductivity indicator values in regions of

Reed Maxwell 2/2/2015 5:06 AM

Deleted: for

Reed Maxwell 2/2/2015 5:06 AM

Deleted: was constructed

Reed Maxwell 2/2/2015 5:06 AM

Deleted: 1km

244 steeper slope. Figure 1e maps the final conductivity values used for simulation. Note that this  
245 complex subsurface dataset is assembled from many sources, and is subject to uncertainty. As  
246 such there are breaks across dataset boundaries, commonly at State or Province and International  
247 political delineations. The fidelity and resolution of the source information used to formulate this  
248 dataset also changes across these boundaries yielding some interfaces in property values.

249 All input datasets are a work in progress and should be continually improved. However,  
250 we feel it is important to continue numerical experiments with the data that is currently available,  
251 while keeping in mind the limitations associated with every model input. Shortcomings in  
252 hydrogeological data sets reflect the lack of detailed unified hydrogeological information that  
253 can be applied in high resolution continental models. This constitutes a significant source of  
254 uncertainty, which needs to be assessed, quantified and ultimately reduced in order to arrive at  
255 precise predictions. Still, it should be noted that the purpose of this work is to demonstrate the  
256 feasibility of integrated modeling to explicitly represent processes across many scales of spatial  
257 variability. By focusing on large-scale behaviors and relationships we limit the impact uncertain  
258 inputs.

259 No-flow boundary conditions were imposed on all sides of the model except the land  
260 surface, where the free-surface overland flow boundary condition was applied. For the surface  
261 flux, a Precipitation-Evapotranspiration (P-E, or potential recharge) product was derived from a  
262 combination of precipitation and model-simulated evaporation and transpiration fluxes for a  
263 product very similar to Maurer et al. (2002), shown in Figure 1d. The model was initialized dry  
264 and the P-E forcing was applied continuously at the land surface until the balance of water  
265 (difference between total outflow and P-E) was less than 3% of storage. For all simulations a

Reed Maxwell 2/2/2015 5:06 AM

Deleted: .

Reed Maxwell 2/2/2015 5:06 AM

Deleted:

Reed Maxwell 2/2/2015 5:06 AM

Deleted: Still

Reed Maxwell 2/2/2015 5:06 AM

Deleted: modeling

Reed Maxwell 2/2/2015 5:06 AM

Deleted: to understand

Reed Maxwell 2/2/2015 5:06 AM

Deleted: and assess their impact on

Reed Maxwell 2/2/2015 5:06 AM

Deleted: predictions

Reed Maxwell 2/2/2015 5:06 AM

Deleted: and

274 | [nonlinear tolerance of  \$10^{-5}\$  and a linear tolerance of  \$10^{-10}\$  were used to ensure proper model](#)  
275 | [convergence.](#)

276 | While this study employs state of the art modeling techniques, it is important to note that  
277 | the numerical simulation of this problem is [far from being](#) trivial. Simulations were split over  
278 | 128 divisions in the  $x$ -direction and 128 in the  $y$ -direction and run on 16,384 compute-cores of an  
279 | IBM BG/Q supercomputer (JUQUEEN) located at the Jülich Supercomputing Centre, Germany.  
280 | These processor splits resulted in approximately 2,000 unknowns per compute core; a relatively  
281 | small number, yet ParFlow's scaling was still good ([better than 60% efficiency](#)) due to the non-  
282 | symmetric preconditioner used (Maxwell 2013). [The reason for this is the special architecture of](#)  
283 | [JUQUEEN with only 256MB of memory per core and relatively slow clock rate.](#) Additionally,  
284 | code performance was improved using efficient preconditioning of the linear system (Osei-  
285 | Kuffuor et al.). The steady-state flow field was accomplished over several steps. Artificial  
286 | dampening was applied to the overland flow equations early in the simulation during water table  
287 | equilibration. Dampening was subsequently decreased and removed entirely as simulation time  
288 | progressed. Large time steps (10,000h) were used initially and were decreased (to 1h) as the  
289 | stream network formed and overland flow became more pronounced with reduced dampening.  
290 | The entire simulation utilized approximately 2.5M core hours of compute time, which resulted in  
291 | less than 1 week of wall-clock time (approximately 150 hours) given the large core counts and  
292 | batch submission process.

293 | Model results were [checked for plausibility](#) against available observations of streamflow  
294 | and hydraulic head (the sum of pressure head and gravitational potential). Observed streamflow  
295 | values were extracted from a spatial dataset of current and historical U.S. Geological Survey  
296 | (USGS) stream gages mapped to the National Hydrography Dataset (NHD) (Stewart et al.,

Reed Maxwell 2/2/2015 5:06 AM

Deleted: still non-

Reed Maxwell 2/2/2015 5:06 AM

Deleted: validated



299 2006). The entire dataset includes roughly 23,000 stations, of which just over half (13,567) fall  
300 within the CONUS domain. For each station, the dataset includes location, drainage area,  
301 sampling time period and flow characteristics including minimum, maximum, mean and a range  
302 of percentiles (1, 5, 10, 20, 25, 50, 75, 80, 90, 95, 99) compiled from the USGS gage  
303 records. For comparison, stations without a reported drainage area, stations not located on or  
304 adjacent to a river cell in ParFlow, and stations whose drainage area were not within twenty  
305 percent of the calculated ParFlow drainage area were filtered out. This resulted in 4,736 stations  
306 for comparison. The 50<sup>th</sup> percentile values for these stations are shown in Figure 2a. Note that  
307 these observations are not naturalized, i.e. no attempt is made to remove dams and diversions  
308 along these streams and rivers, however some of these effects will be minimized given the longer  
309 temporal averages. Hydraulic head observations of groundwater at more than 160,000 locations  
310 were assembled by Fan et al. (Fan et al. 2007; Fan et al. 2013). Figure 2b plots the  
311 corresponding water table depth at each location calculated as the difference between elevation  
312 and hydraulic head. Note that these observations include groundwater pumping (most wells are  
313 drilled for extraction rather than purely observation).

## 315 Results and Discussion

316 Figures 3 and 4 plot simulated streamflow and water table depth, respectively, over much  
317 of continental North America, both on a log scale for flow (Figure 3) and water table depth  
318 (Figure 4). Figure 3 shows a complex stream network with flow rates spanning many orders of  
319 magnitude. Surface flows originate in the headwaters (or recharge zones) creating tributaries that  
320 join to form the major river systems in North America. Note, as discussed previously that the  
321 locations for flowing streams are not enforced in ParFlow but form due to ponded water at the

Reed Maxwell 2/2/2015 5:06 AM  
Deleted:

Reed Maxwell 2/2/2015 5:06 AM  
Deleted: -

Reed Maxwell 2/2/2015 5:06 AM  
Deleted: -  
Reed Maxwell 2/2/2015 5:06 AM  
Formatted: Indent: First line: 0.5"

325 surface (i.e. values of  $h > 0$  in the top layer of the model in Equations 1-3). Overland flow is  
326 promoted both by topographic convergence, and surface and subsurface flux; however, with this  
327 formulation there is no requirement that all potential streams support flow. Thus, the model,  
328 captures the generation of the complete stream network without specifying the presence and  
329 location of rivers in advance, but rather by allowing channelized flow to evolve as a result of  
330 explicitly simulated non-linear physical processes.

331 The insets in Figure 3 demonstrate multiscale detail ranging from the continental river  
332 systems to the first-order headwaters. In Figure 4, water table depth also varies over five orders  
333 of magnitude. Whereas aridity drives large-scale differences in water table depth (Figure 1d), at  
334 smaller scales, lateral surface and subsurface flow processes clearly dominate recharge and  
335 subsurface heterogeneity (see insets to Figure 4). Water tables are deeper in the more arid  
336 western regions, and shallower in the more humid eastern regions of the model. However, areas  
337 of shallow water table exist along arid river channels and water table depths greater than 10m  
338 exist in more humid regions. Note that this is a pre-development simulation, thus, results do not  
339 include any anthropogenic water management features such as groundwater pumping, surface  
340 water reservoirs, irrigation or urbanization, all of which are present in the observations. Many  
341 of these anthropogenic impacts have been implemented into the ParFlow modeling framework  
342 (Ferguson and Maxwell 2011; Condon and Maxwell 2013; Condon and Maxwell 2014). While  
343 anthropogenic impacts are clearly influential on water resources, a baseline simulation allows for  
344 a comparison between the altered and unaltered systems in future.

345 Next we compare the results of the numerical experiment to observations. As noted  
346 previously, this is not a calibrated model. Therefore, the purpose of these comparisons is to  
347 provide a plausibility check of model behavior and physical processes. Figure 5 plots observed

Reed Maxwell 2/2/2015 5:06 AM

Deleted: novelty

Reed Maxwell 2/2/2015 5:06 AM

Deleted: , although many

350 and simulated hydraulic head and streamflow for the dataset shown in Figure 2. Hydraulic head  
351 (Figure 5a) is plotted (as opposed to water table depth) as it is the motivating force for lateral  
352 flow in the simulation; it includes both the topography and pressure influences on the final  
353 solution. We see a very close agreement between observations and model simulations, though  
354 given the large range in hydraulic heads the goodness of fit may be somewhat [driven by the](#)  
355 [underlying topography](#). Additional metrics and comparisons are explored below. Simulated  
356 streamflow (Figure 5b) also agrees closely with observations. There is some bias, particularly  
357 for smaller flows, [\(which we emphasize by plotting in log scale\)](#), which also exhibit more scatter  
358 than larger flows, and [are likely](#) due to the 1km grid resolution employed here. Larger flows are  
359 more integrated measures of the system and might be less sensitive to resolution or local  
360 heterogeneity in model parameters. [We see this when linear least squared statistics are computed](#)  
361 [where the  \$R^2\$  value increases to 0.8.](#)

362 Figure 6 plots histograms of predicted and observed water table depth (a), hydraulic head  
363 (b), median (50th percentile) flow and 75th percentile flows (c-d). The hydraulic head shows  
364 good agreement between simulated and observed (Figure 6b). While hydraulic head is the  
365 motivation for lateral flow and has been used in prior comparisons (e.g. Fan et al 2007) both  
366 observed and simulated values are highly dependent on the local elevation. Figure 6a plots the  
367 water table depth below ground surface, or the difference between local elevation and  
368 groundwater. Here we see the simulated water table depths are shallower than the observed,  
369 something observed in prior simulations of large-scale water table depth (Fan et al 2013). The  
370 observed water tables may include anthropogenic impacts, namely groundwater pumping, while  
371 the model simulations do not and this is a likely cause for this difference. Also, because  
372 groundwater wells are usually installed for extraction purposes there is no guarantee that the

Reed Maxwell 2/2/2015 5:06 AM

Deleted: obscured.

Reed Maxwell 2/2/2015 5:06 AM

Deleted: ,

Reed Maxwell 2/2/2015 5:06 AM

Deleted: may be

376 groundwater observations are an unbiased sample of the system as a whole. Figure 6c plots the  
377 steady-state derived flow values compared to median observed flow values and Figure 6d plots  
378 these same steady-state simulated flows compared to the 75th percentile of the observed transient  
379 flow at each station. While the ParFlow model provides a robust representation of runoff  
380 generation processes, the steady-state simulations average event flows. We see the model  
381 predicts greater flow than the 50th percentile observed flows (Figure 6c) and good agreement  
382 between the model simulations and the 75th percentile observed flows (Figure 6d). This  
383 indicates a potentially wet bias in the forcing, which might also explain the shallower water table  
384 depths.

385        Figures 7 and 8 compare observed and simulated flows and water table depths for each of  
386 the major basin encompassed by the model. Water tables are generally predicted to be shallower  
387 in the model than observations with the exception of the Upper and Lower Colorado which  
388 demonstrate better agreement between model simulations and observations than other basins.  
389 These histograms agree with a visual inspection of Figures 2b and 4 which also indicate deeper  
390 observed water tables. Figure 8 indicates that simulated histograms of streamflow also predict  
391 more flow than the observations. This might indicate that the P-E forcing is too wet. However,  
392 a comparison of streamflow for the Colorado [Watershed](#), where water table depths agree ([Figure](#)  
393 [8 e and g](#)) and flows are overpredicted, ([Figure 7 e and g](#)), indicates a more complex set of  
394 interactions than basic water balance driven by forcing.

395        To better diagnose model processes, model inputs are compared with model simulation  
396 outputs over example regions chosen to isolate the impact of topographic slope, forcing and  
397 hydraulic conductivity on subsurface-surface water hydrodynamics. [We do this as a check to see](#)  
398 [if and how this numerical experiment compares to real observations. It is important to use a](#)

Reed Maxwell 2/2/2015 5:06 AM

Deleted: ,

400 [range of measures of success that might be different from that used in a model calibration where](#)  
401 [inadequacies in model parameters and process might be muted while tuning the model to better](#)  
402 [match observations](#). Figure 9 juxtaposes slope, potential recharge, surface flow, water table  
403 depth, hydraulic conductivity and a satellite image composite also at 1km resolution (the NASA  
404 Blue Marble image, (Justice et al. 2002)) and facilitates a visual diagnosis of control by the three  
405 primary model inputs. While the model was run to steady-state and ultimately all the potential  
406 recharge has to exit the domain as discharge, the distribution and partitioning between  
407 groundwater and streams depends on the slope and hydraulic conductivity. Likewise, while  
408 topographic lows create the potential for flow convergence, it is not a model requirement that  
409 [these will develop into stream loci](#). Figure 9 demonstrates some of these relationships quite  
410 clearly over a portion of the model that transitions from semi-arid to more humid conditions as  
411 the North and South Platte River systems join the Missouri. As expected changes in slope yield  
412 flow convergence, however, this figure also shows that as recharge increases from west to east  
413 ( $X > 1700$  km, panel c) the model generally predicts shallower water tables and greater stream  
414 density (panels d and e, respectively). Conversely, in localized areas of decreased P-E (e.g.  $700$   
415  $< Y < 900$  km specifically south of the Platte River) water tables increase and stream densities  
416 decrease. The satellite image (panel f) shows increases in vegetation that correspond to  
417 shallower water tables and increased stream density.

418 Hydraulic conductivity also has a significant impact on water table depth and stream  
419 network density. In areas of greater recharge in the eastern portion of Figure 9c, regions with  
420 larger hydraulic conductivity (panel b) show decreased stream network density and increased  
421 water table depths. This [is](#) more clearly demonstrated in Figure 10 (a region in the upper  
422 Missouri) where, except for the northeast corner, recharge is uniformly low. Slopes are also

Reed Maxwell 2/2/2015 5:06 AM

Deleted: this create a

Reed Maxwell 2/2/2015 5:06 AM

Deleted: , somewhat counter intuitively,

425 generally low (panel a), yet hydraulic conductivities show a substantial increase due to a change  
426 in datasets between state and country boundaries (panel b,  $X > 1250\text{km}$ ,  $Y > 1400\text{ km}$ ). The  
427 relative increase in hydraulic conductivity decreases hydraulic gradients under steady state  
428 conditions and generally increases water table depth, which in turn decreases stream network  
429 density. This change in hydraulic conductivity yields a decrease in the formation of stream  
430 networks resulting in an increase in water table depth. Thus, hydraulic conductivity has an  
431 important role in partitioning moisture between surface and subsurface flow, [also](#) under steady-  
432 state conditions. While mass balance requires that overall flow must be conserved, larger  
433 conductivity values allow this flow to be maintained within the subsurface while lower  
434 conductivities force the surface stream network to maintain this flow. In turn, stream networks  
435 connect regions of varying hydrodynamic conditions and may result in locally infiltrating  
436 conditions creating a losing-stream to recharge groundwater. This underscores the connection  
437 between input variables and model predictions, an equal importance of hydraulic conductivity to  
438 recharge in model states and the need to continually improve input datasets.

439 Finally, the connection between stream flow and drainage area is a classical scaling  
440 relationship (Rodriguez-Iturbe and Rinaldo 2001), which usually takes the power law form  
441  $Q = kA^n$ , where  $Q$  is volumetric streamflow [ $\text{L}^3\text{T}^{-1}$ ],  $A$  is the contributing upstream area [ $\text{L}^2$ ] and  $k$   
442 [ $\text{LT}^{-1}$ ] and  $n$  are empirical constants. While this relationship has been demonstrated for  
443 individual basins and certain flow conditions (Rodriguez-Iturbe and Rinaldo 2001), generality  
444 has not been established (Glaster 2009). Figure [11a](#) plots simulated streamflow as a function of  
445 associated drainage area on log-log axes, and Figure [11b](#) plots the same variables for median  
446 observed streamflow from more than 4,000 gaging stations. While no single functional  
447 relationship is evident from this plot, there is a striking maximum limit of flow as a function of

Reed Maxwell 2/2/2015 5:06 AM

Deleted: even

Reed Maxwell 2/2/2015 5:06 AM

Deleted: 10a

Reed Maxwell 2/2/2015 5:06 AM

Deleted: 10b

451 drainage area with a continental scaling coefficient of  $n = 0.84$ . Both Figures [11a](#) and b are  
452 colored by aridity index (AI), the degree of dryness of a given location. Color gradients that  
453 transition from blue (more humid) to red (more arid) show that humid basins fall along the  
454 maximum flow-discharge line, while arid basins have less discharge and fall below this line. For  
455 discharge observations (Figure [11b](#)) the same behavior is observed, where more humid stations  
456 fall along the  $n=0.9$  line and more arid stations fall below this line. Essentially this means that in  
457 humid locations, where water is not a limiting factor, streamflow scales most strongly with  
458 topography and area. Conversely arid locations fall below this line because flow to streams is  
459 limited by groundwater storage.

Reed Maxwell 2/2/2015 5:06 AM

Deleted: 10a

Reed Maxwell 2/2/2015 5:06 AM

Deleted: 10b

## 461 Conclusions

462 Here we present the results of an integrated, multiphysics-based hydrologic simulation  
463 covering much of Continental North America at hyperresolution (1km). This [numerical](#)  
464 [experiment](#) provides a consistent theoretical framework for the analysis of groundwater and  
465 surface water interactions and scaling from the headwaters to continental scale ( $10^0$ - $10^7$  km<sup>2</sup>).  
466 The framework exploits high performance computing to meet this grand challenge in hydrology  
467 (Wood et al. 2011; Gleeson and Cardiff 2014; Bierkens et al. 2015). We demonstrate that  
468 continental-scale, integrated hydrologic models are feasible and can reproduce observations and  
469 the essential features of streamflow and groundwater. Results show that scaling of surface flow  
470 is related to both drainage area and aridity. These results may be interrogated further to  
471 understand the role of topography, subsurface properties and climate on groundwater table and  
472 streamflow, and used as a platform to diagnose scaling behavior, e.g. surface flow from the  
473 headwaters to the continent.

Reed Maxwell 2/2/2015 5:06 AM

Deleted: simulation

477        These presented results are a first-step in high resolution, integrated, continental-scale  
478        simulation. We simulate an unaltered, or pre-development scenario of groundwater and surface  
479        water flows under steady-state conditions. As such, the discussion focuses on the physical  
480        controls of groundwater surface water interactions and scaling behavior; however there are  
481        obvious limitations to this scenario and these simulations. Clearly reservoir management,  
482        groundwater pumping, irrigation, diversion and urban expansion all shape modern hydrology.  
483        Work has been undertaken to include these features within the ParFlow framework at smaller  
484        scales (Ferguson and Maxwell 2011; Ferguson and Maxwell 2012; Condon and Maxwell 2013;  
485        Condon and Maxwell 2014) and an important next step is to scale the impacts out to the  
486        continent.

487        Additionally, the steady-state simulation does not take into consideration temporal  
488        dynamics or complex land-surface processes, also important in determining the quantity and  
489        fluxes of water. These limitations can all be addressed within the current modeling framework  
490        but require transient simulations and additional computational resources. Model performance is  
491        also limited by the quality of available input datasets. As noted throughout the discussion,  
492        existing datasets are subject to uncertainty and are clearly imperfect. As improved subsurface  
493        characterization becomes available, this information can be used to better inform models and  
494        fully understand the propagation of uncertainty in these types of numerical experiments (e.g.  
495        Maxwell and Kollet 2008; Kollet 2009). However, while the magnitudes of states and fluxes may  
496        change with improved datasets, the overall trends and responses predicted here are not likely to  
497        change within the confines of the numerical experiment. While there are always improvements  
498        to be made, these simulations represent a critical first step in understanding coupled surface

Reed Maxwell 2/2/2015 5:06 AM  
Deleted: .

Reed Maxwell 2/2/2015 5:06 AM  
Deleted: .

Reed Maxwell 2/2/2015 5:06 AM  
Deleted: .

Reed Maxwell 2/2/2015 5:06 AM  
Deleted: .



503 subsurface hydrologic processes and scaling at [continental scales resolving variances over four](#)  
504 [for orders of spatial scales](#).

Reed Maxwell 2/2/2015 5:06 AM

Deleted: large

Reed Maxwell 2/2/2015 5:06 AM

Deleted: extent

505 This study highlights the utility of high performance computing in addressing the grand  
506 challenges in hydrological sciences and represents an important advancement in our  
507 understanding of hydrologic scaling in continental river basins. By providing an integrated  
508 model we open up a useful avenue of research to bridge physical processes across spatial scales  
509 in a hydrodynamic, physics-based upscaling framework.

510

#### 511 **Code Availability**

512 ParFlow is an open-source, modular, parallel integrated hydrologic platform freely available via  
513 the GNU LGPL license agreement. ParFlow is developed by a community led by the Colorado  
514 School of Mines and F-Z Jülich with contributors from a number of other institutions. Specific  
515 versions of ParFlow are archived with complete documentation and may be downloaded<sup>1</sup> or  
516 checked-out from a commercially hosted, free SVN repository: [v3, r693 was the version used in](#)  
517 [this study](#). The input data and simulations presented here will be made available and may be  
518 obtained by contacting the lead author via email.

Reed Maxwell 2/2/2015 5:06 AM

Deleted: .

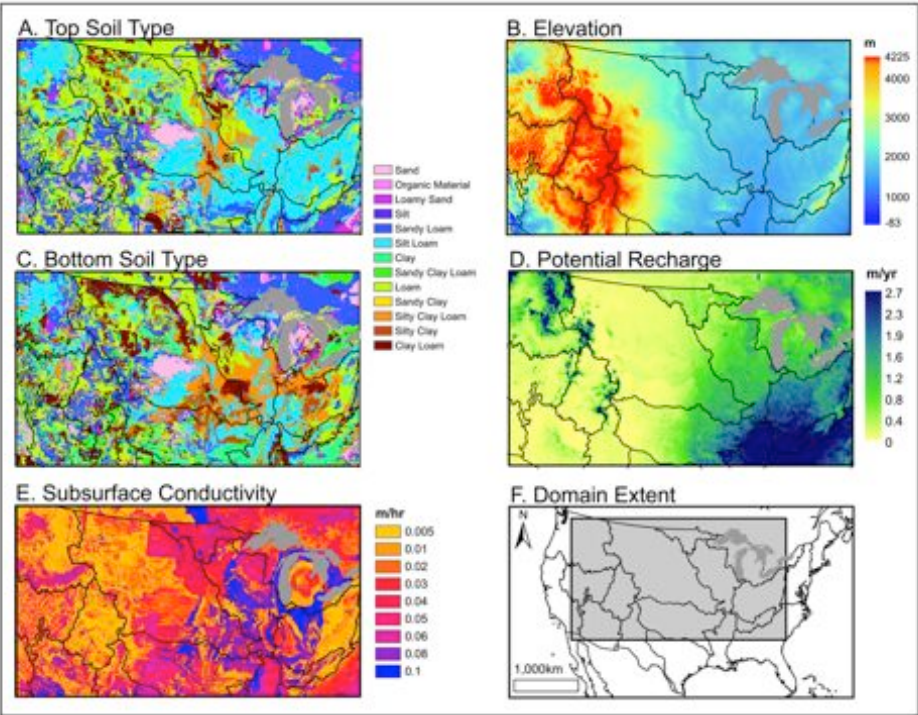
519

---

<sup>1</sup> [http://inside.mines.edu/~rmaxwell/maxwell\\_software.shtml](http://inside.mines.edu/~rmaxwell/maxwell_software.shtml)

523

524 **Figures**



525  
526 Figure 1. Maps of top soil type (a), elevation (masl) (b), bottom soil type (c), potential recharge,  
527 P-E, (m/y) (d), saturated hydraulic conductivity (m/h) (e) over the model domain (f).  
528

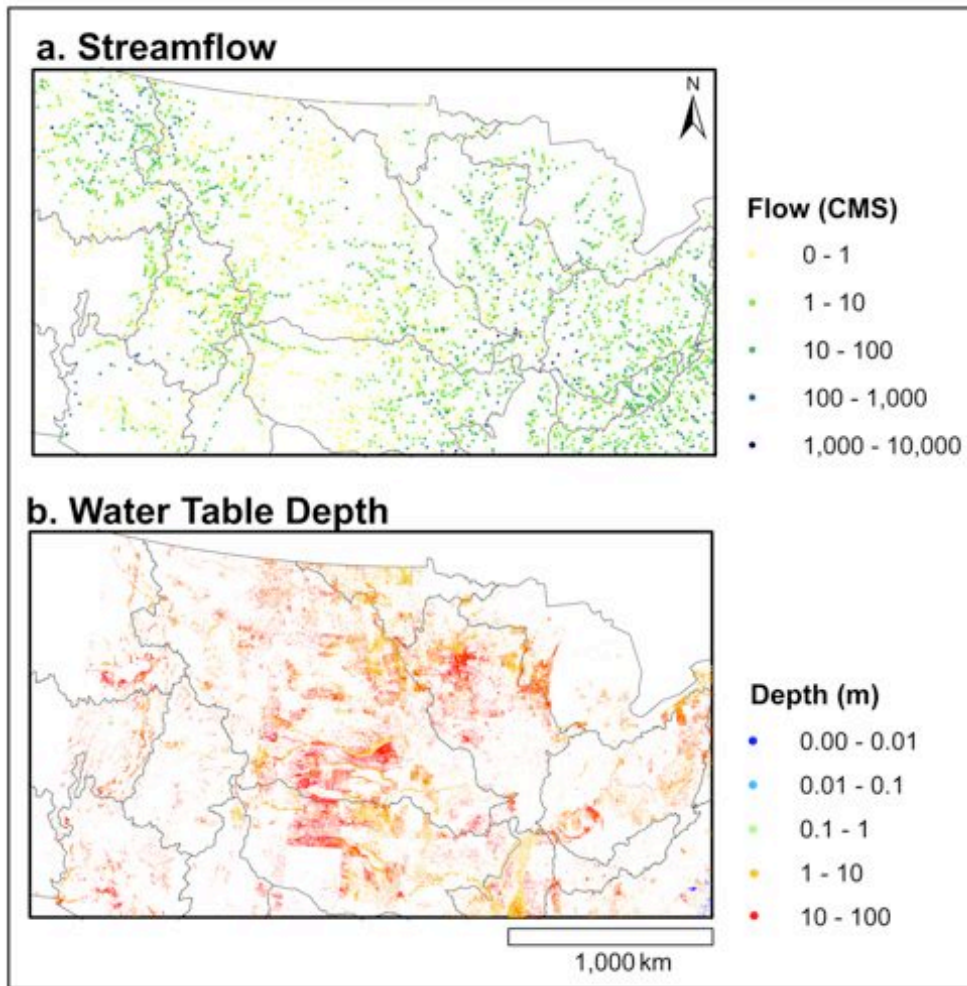
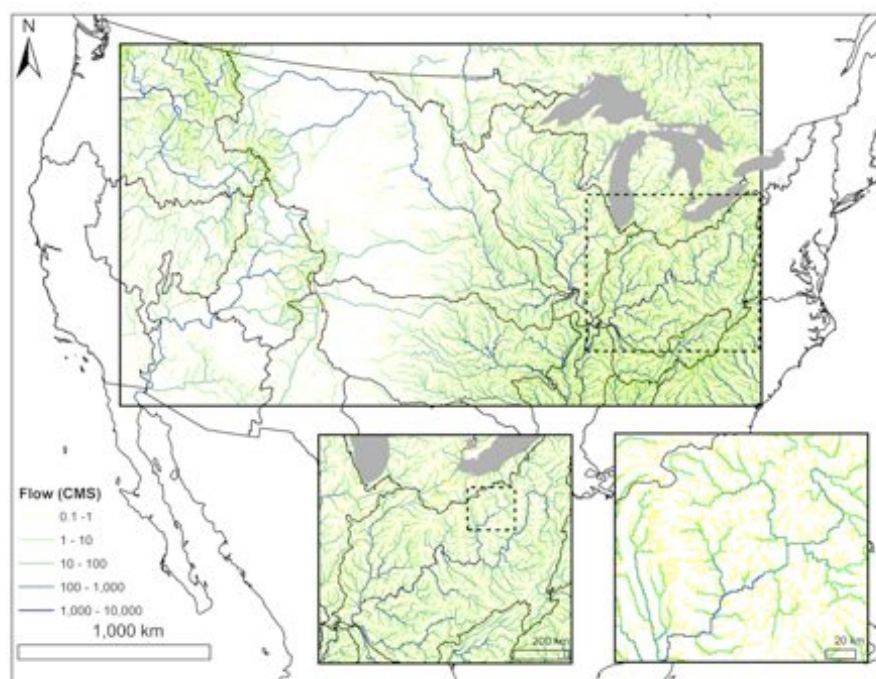


Figure 2. Plot of observed streamflow (a) and observed water table depth (b).



532  
 533 Figure 3. Map of simulated surface flow ( $\text{m}^3/\text{s}$ ) over the CONUS domain with two insets  
 534 zooming into the Ohio river basin. Colors represent surface flow in log scale and line widths  
 535 vary slightly with flow for the first two panels.  
 536

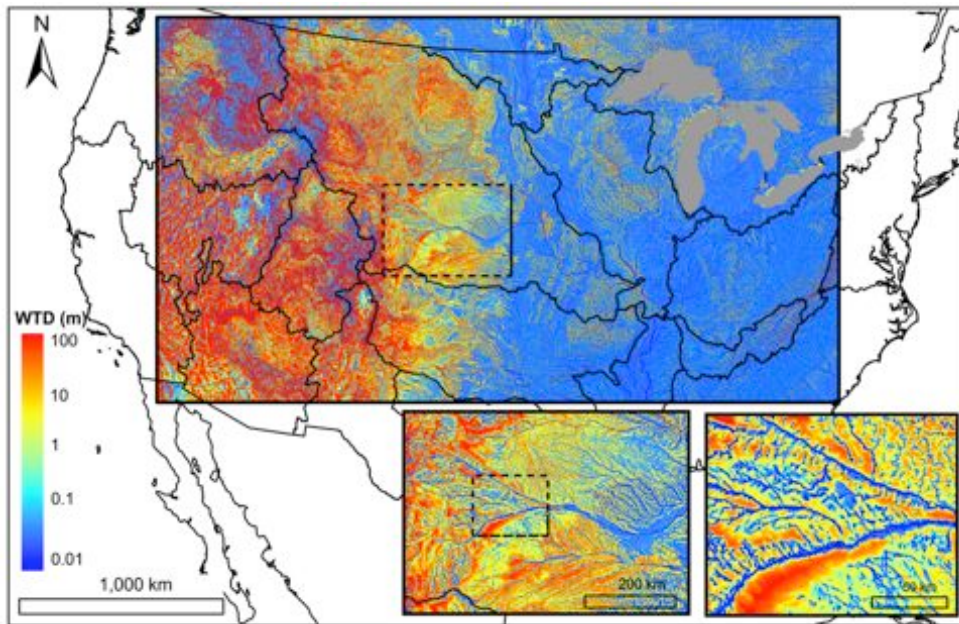
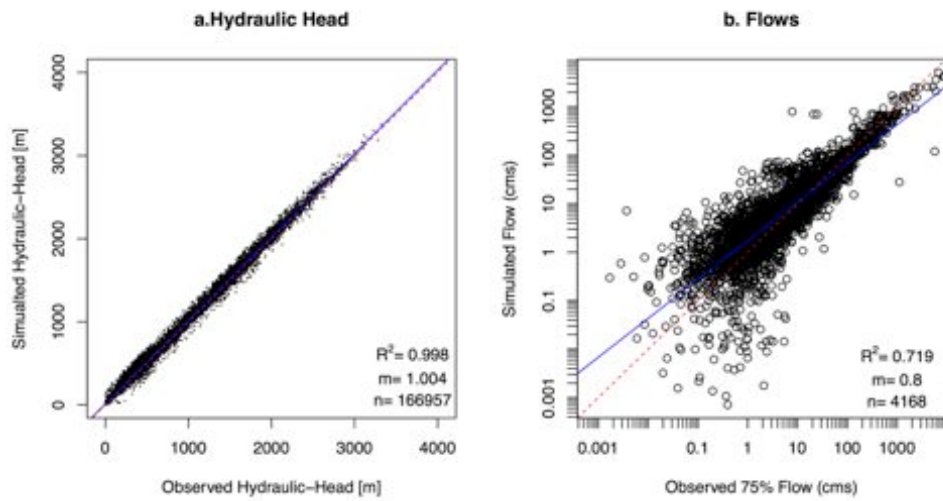


Figure 4. Map of water table depth (m) over the simulation domain with two insets zooming into the North and South Platte River basin, headwaters to the Mississippi. Colors represent depth in log scale (from 0.01 to 100m).



542

543 Figure 5. Scatterplots of simulated v. observed hydraulic head (a) and surface flow (b).

544

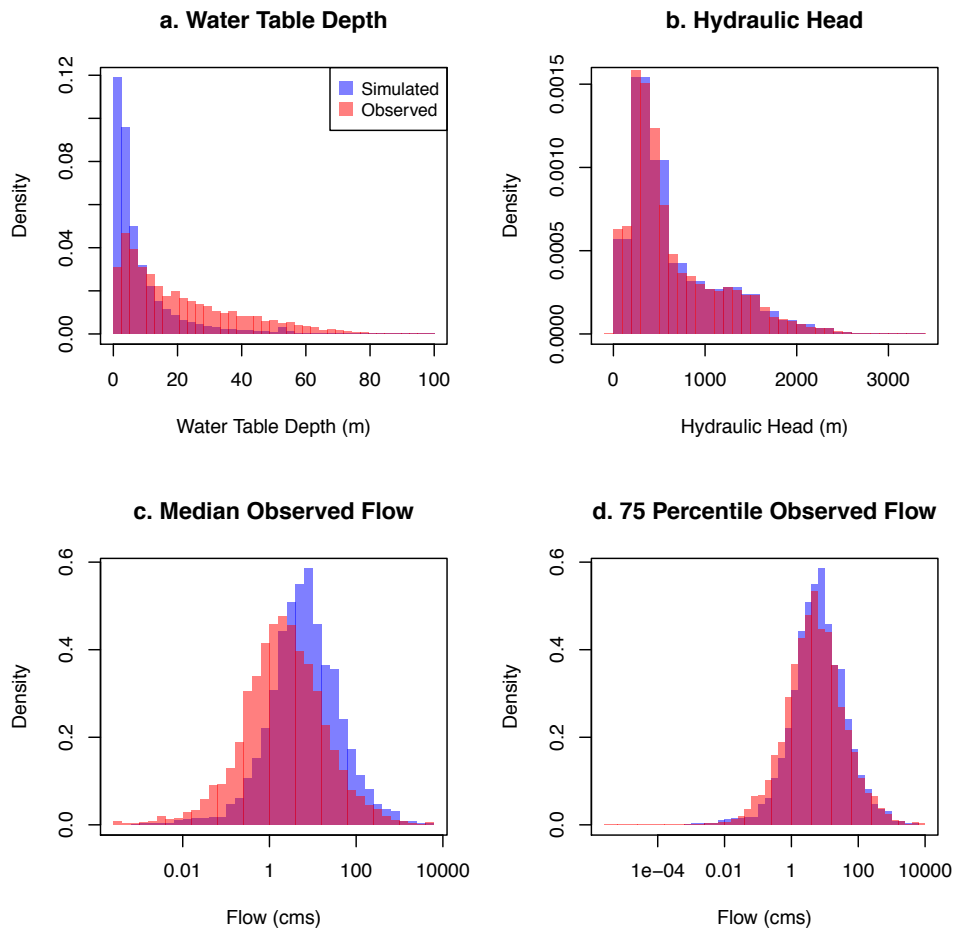
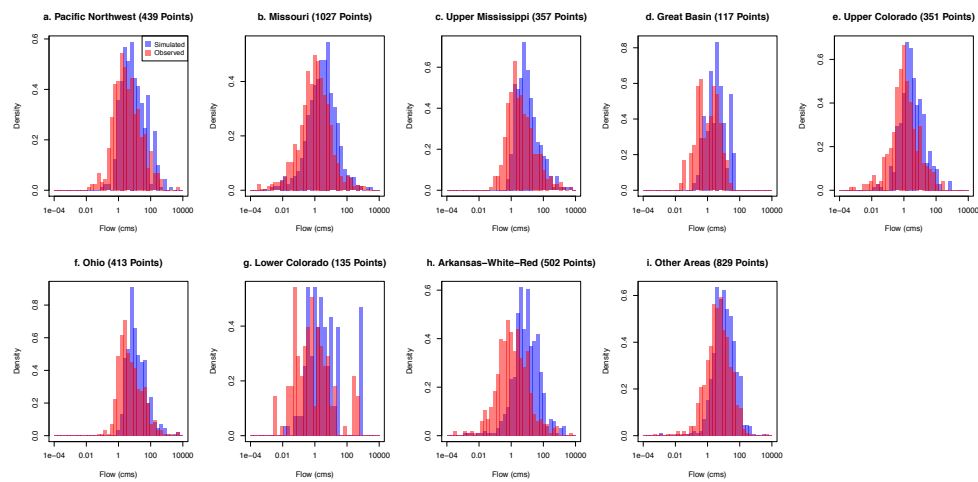


Figure 6. Histograms of simulated and observed water table depth (a), hydraulic head (b), median observed flow (c) and 75<sup>th</sup> percentile observed flow (d).



549  
550



551  
552  
553

Figure 7. Distributions of observed and simulated streamflow by basin as indicated.



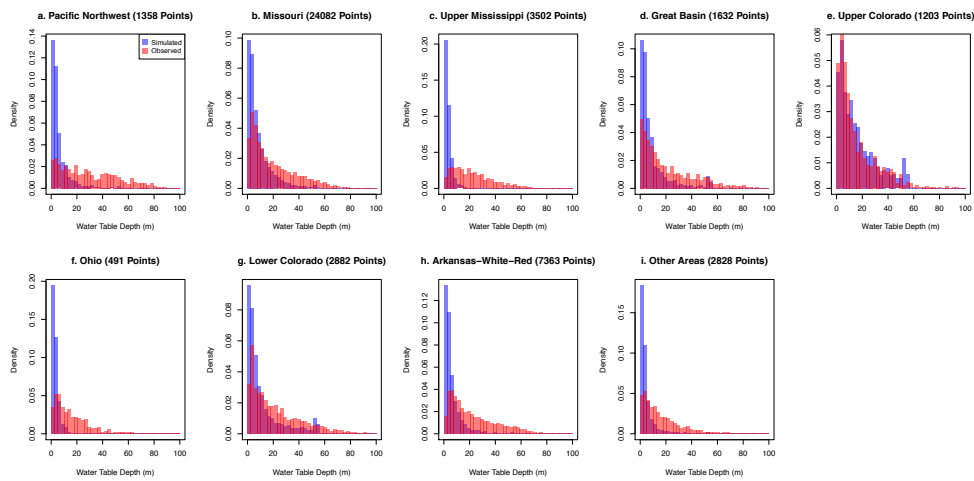


Figure 8. Distributions of observed and simulated water table depth by basin as indicated.

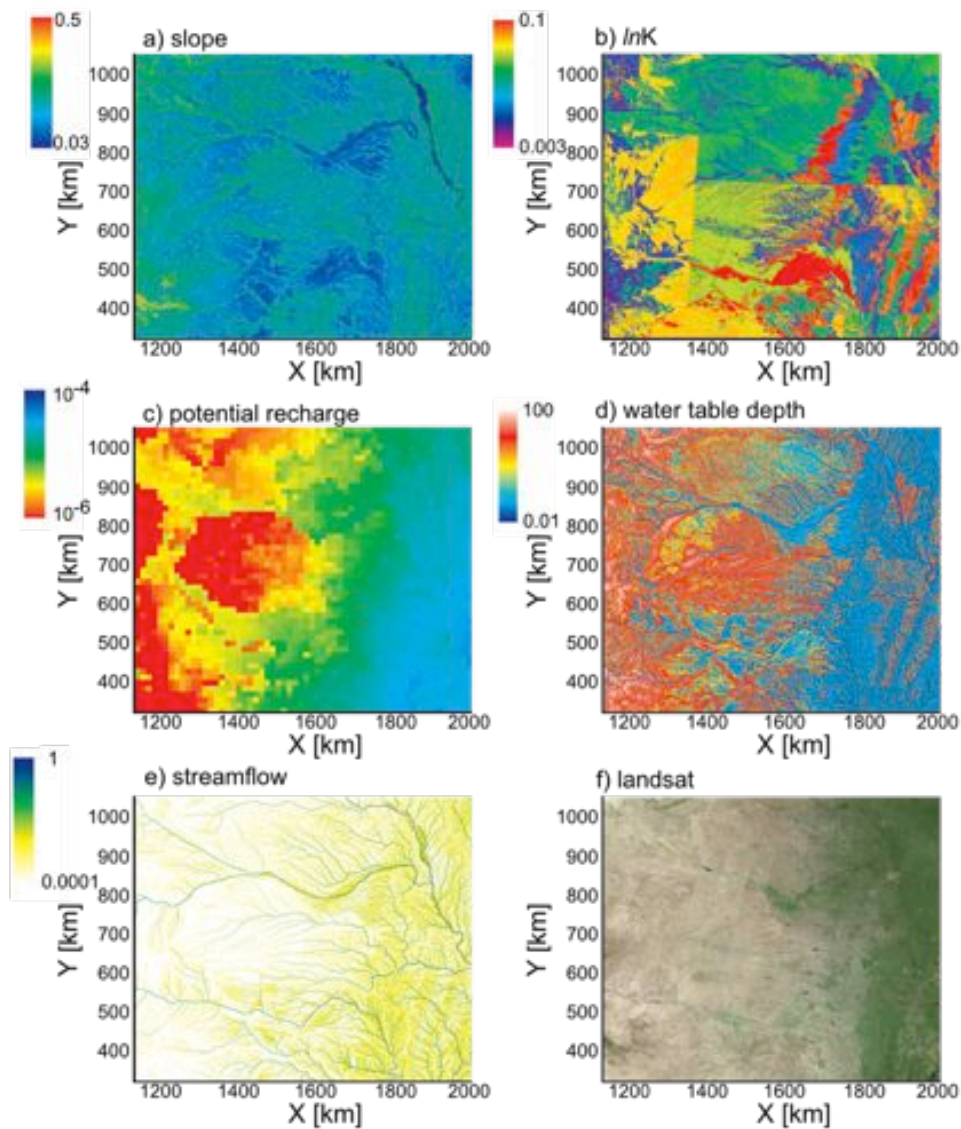
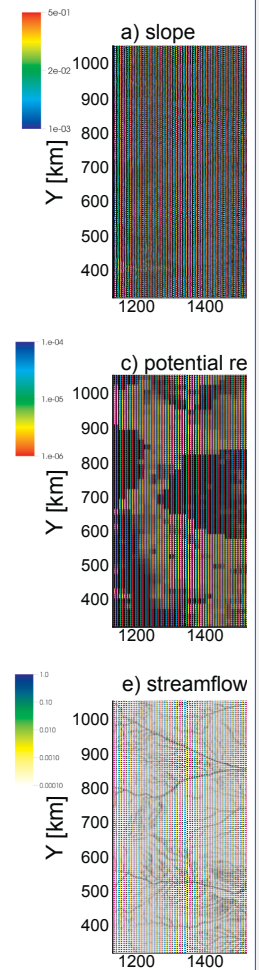


Figure 9. Plots of topographic slope (a), hydraulic conductivity (b) potential recharge (c), water table depth (d), streamflow (e) and satellite image (f) for a region of the model covering the Platte River basin.

Reed Maxwell 2/2/2015 5:06 AM



Deleted:

Reed Maxwell 2/2/2015 5:06 AM

Deleted:

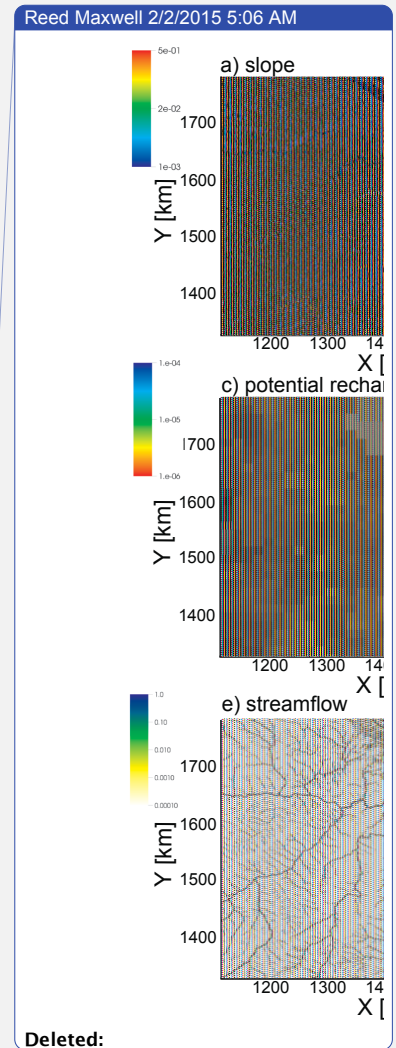
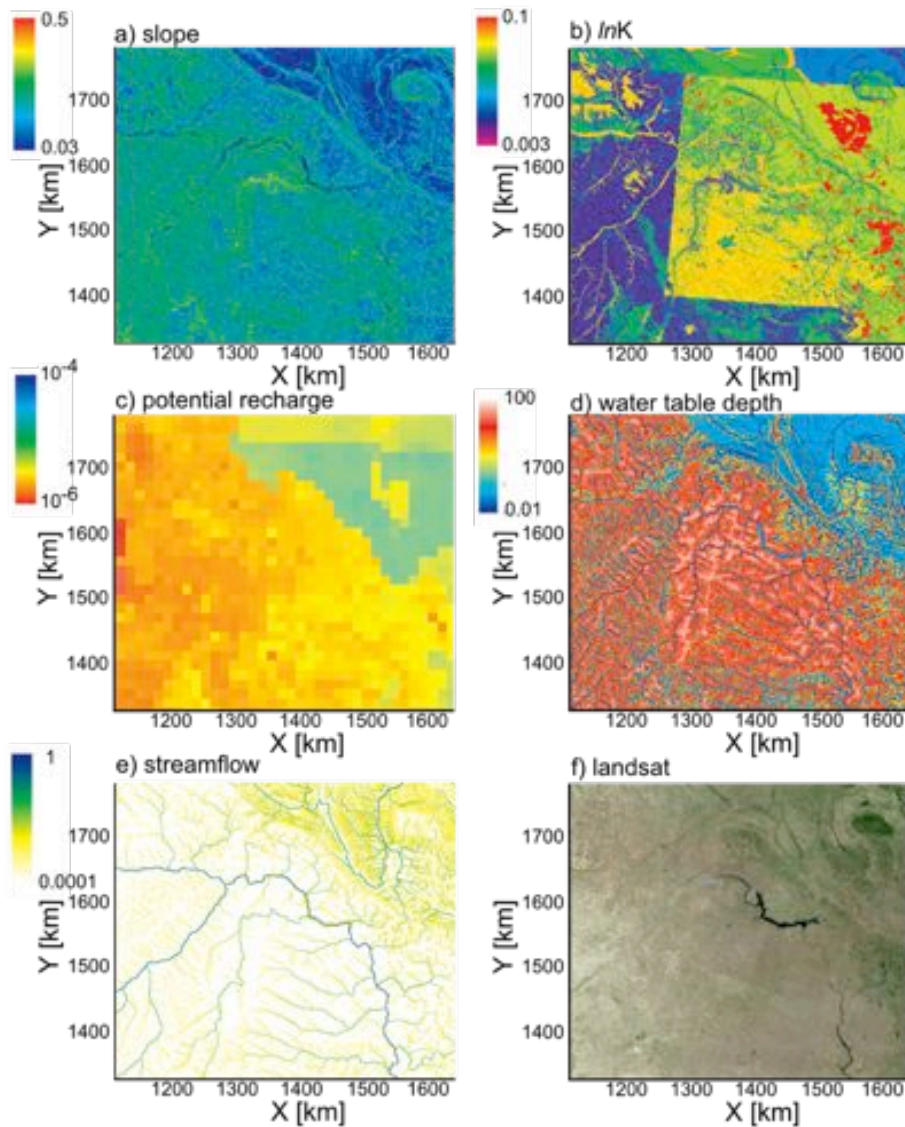


Figure 10. Plots of topographic slope (a), hydraulic conductivity (b) potential recharge (c), water table depth (d), streamflow (e) and satellite image (f) for a region of the model covering the Upper Missouri basin.

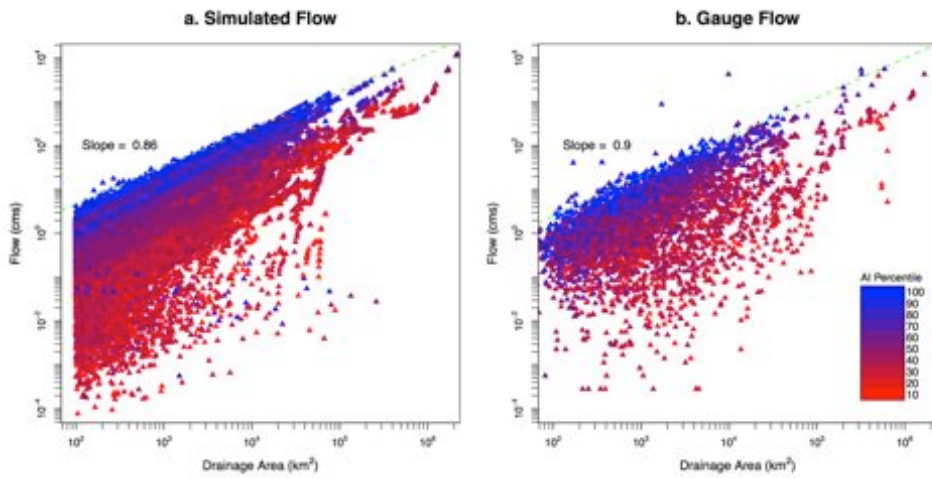


Figure 11. Plots of scaling relationships for simulated and median observed surface flow. Log-scale plots of surface flow as a function of contributing drainage area derived from the model simulation (a) and observations (b). Individual symbols are colored by aridity index (AI) with blue colors being humid and red colors being arid in panels (a) and (b).



## References

- Anyah, R. O., C. P. Weaver, G. Miguez-Macho, Y. Fan and A. Robock (2008). "Incorporating water table dynamics in climate modeling: 3. Simulated groundwater influence on coupled land-atmosphere variability." *Journal of Geophysical Research-Atmospheres* **113**(D7): 15,
- Ashby, S. F. and R. D. Falgout (1996). "A parallel multigrid preconditioned conjugate gradient algorithm for groundwater flow simulations." *Nuclear Science and Engineering* **124**(1): 145-159,
- Beven, K. (2004). "Robert e. Horton's perceptual model of infiltration processes." *Hydrological Processes* **18**(17): 3447-3460,
- Bierkens, M. F. P., V. A. Bell, P. Burek, N. Chaney, L. E. Condon, C. H. David, A. de Roo, P. Döll, N. Drost, J. S. Famiglietti, M. Flörke, D. J. Gochis, P. Houser, R. Hut, J. Keune, S. Kollet, R. M. Maxwell, J. T. Reager, L. Samaniego, E. Sudicky, E. H. Sutanudjaja, N. van de Giesen, H. Winsemius and E. F. Wood (2015). "Hyper-resolution global hydrological modelling: What is next?" *Hydrological Processes* **29**(2): 310-320, [10.1002/hyp.10391](https://doi.org/10.1002/hyp.10391)
- Camporese, M., C. Paniconi, M. Putti and S. Orlandini (2010). "Surface-subsurface flow modeling with path-based runoff routing, boundary condition-based coupling, and assimilation of multisource observation data." *Water Resources Research* **46**(2): W02512, [10.1029/2008wr007536](https://doi.org/10.1029/2008wr007536)
- Camporese, M., C. Paniconi, M. Putti and S. Orlandini (2010). "Surface-subsurface flow modeling with path-based runoff routing, boundary condition-based coupling, and assimilation of multisource observation data." *Water Resour. Res.* **46**(2): W02512, doi: [10.1029/2008wr007536](https://doi.org/10.1029/2008wr007536)
- Camporese, M., D. Penna, M. Borga and C. Paniconi (2014). "A field and modeling study of nonlinear storage-discharge dynamics for an alpine headwater catchment." *Water Resources Research* **50**(2): 806-822, [10.1002/2013wr013604](https://doi.org/10.1002/2013wr013604)
- Condon, L. E. and R. M. Maxwell (2013). "Implementation of a linear optimization water allocation algorithm into a fully integrated physical hydrology model." *Advances in Water Resources* **60**(0): 135-147, <http://dx.doi.org/10.1016/j.advwatres.2013.07.012>
- Condon, L. E. and R. M. Maxwell (2014). "Feedbacks between managed irrigation and water availability: Diagnosing temporal and spatial patterns using an integrated hydrologic model." *Water Resources Research* **50**(3): 2600-2616, [10.1002/2013wr014868](https://doi.org/10.1002/2013wr014868)
- Condon, L. E., R. M. Maxwell and S. Gangopadhyay (2013). "The impact of subsurface conceptualization on land energy fluxes." *Advances in Water Resources* **60**(0): 188-203, <http://dx.doi.org/10.1016/j.advwatres.2013.08.001>
- Döll, P., H. Hoffmann-Dobrev, F. T. Portmann, S. Siebert, A. Eicker, M. Rodell, G. Strassberg and B. R. Scanlon (2012). "Impact of water withdrawals from groundwater and surface water on continental water storage variations." - **59**, *Äi60*(- 0): - 156,
- Dunne, T. (1983). "Relation of field studies and modeling in the prediction of storm runoff." *Journal of Hydrology* **65**(1, Äi3): 25-48, [http://dx.doi.org/10.1016/0022-1694\(83\)90209-3](http://dx.doi.org/10.1016/0022-1694(83)90209-3)
- Fan, Y., H. Li and G. Miguez-Macho (2013). "Global patterns of groundwater table depth." *Science* **339**(6122): 940-943, [10.1126/science.1229881](https://doi.org/10.1126/science.1229881)

Reed Maxwell 2/2/2015 5:06 AM

**Deleted:** Camporese, M., C. Paniconi, M. Putti and S. Orlandini (2010). "Surface-subsurface flow modeling with path-based runoff routing, boundary condition-based coupling, and assimilation of multisource observation data." *Water Resour. Res.* **46**(2): W02512, doi: [10.1029/2008wr007536](https://doi.org/10.1029/2008wr007536) .

628 Fan, Y., G. Miguez-Macho, C. P. Weaver, R. Walko and A. Robock (2007). "Incorporating  
 629 water table dynamics in climate modeling: 1. Water table observations and equilibrium  
 630 water table simulations." *Journal of Geophysical Research-Atmospheres* **112**(D10): -,  
 631 Ferguson, I. M. and R. M. Maxwell (2011). "Hydrologic and land-energy feedbacks of  
 632 agricultural water management practices." *Environmental Research Letters* - **6**(- 1),  
 633 doi:10.1088/1748-9326/6/1/014006  
 634 | [Ferguson, I. M. and R. M. Maxwell \(2012\). "Human impacts on terrestrial hydrology: Climate  
 635 change versus pumping and irrigation." \*Environmental Research Letters\* \*\*7\*\*\(4\): 044022.](#)  
 636 Freeze, R. A. and R. L. Harlan (1969). "Blueprint for a physically-based, digitally-simulated  
 637 hydrologic response model." *Journal of Hydrology* **9**: 237-258,  
 638 Glaster, J. C. (2009). "Testing the linear relationship between peak annual river discharge and  
 639 drainage area using long-term usgs river gauging records." *Geological Society of  
 640 America Special Papers* **451**: 159-171, 10.1130/2009.2451(11)  
 641 Gleeson, T. and M. Cardiff (2014). "The return of groundwater quantity: A mega-scale and  
 642 interdisciplinary "future of hydrogeology"?" *Hydrogeology Journal*: **4**, 10.1007/s10040-  
 643 013-0998-8  
 644 Gleeson, T., L. Marklund, L. Smith and A. H. Manning (2011). "Classifying the water table at  
 645 regional to continental scales." *Geophysical Research Letters* **38**(L05401): 6,  
 646 10.1029/2010GL046427  
 647 Gleeson, T., L. Smith, N. Moosdorf, J. Hartmann, H. H. Dürr, A. H. Manning, L. P. H. van Beek  
 648 and A. M. Jellinek (2011). "Mapping permeability over the surface of the earth."  
 649 *Geophysical Research Letters* **38**(2): L02401, 10.1029/2010gl045565  
 650 Goderniaux, P., S. Brouyere, H. J. Fowler, S. Blenkinsop, R. Therrien, P. Orban and A.  
 651 Dassargues (2009). "Large scale surface, subsurface hydrological model to assess  
 652 climate change impacts on groundwater reserves." *Journal of Hydrology* **373**(1, 2):  
 653 122-138, <http://dx.doi.org/10.1016/j.jhydrol.2009.04.017>  
 654 | [Horton, R. E. \(1933\). "The role of infiltration in the hydrologic cycle." \*Transactions-American  
 655 Geophysical Union\* \*\*14\*\*: 446-460.](#)  
 656 Jiang, X., G. Y. Niu and Z. L. Yang (2009). "Impacts of vegetation and groundwater dynamics  
 657 on warm season precipitation over the central united states." *Journal of Geophysical  
 658 Research* **114**: 15,  
 659 Jones, J. E. and C. S. Woodward (2001). "Newton-krylov-multigrid solvers for large-scale,  
 660 highly heterogeneous, variably saturated flow problems." *Advances in Water Resources*  
 661 **24**(7): 763-774,  
 662 Jones, J. P., E. A. Sudicky, A. E. Brookfield and Y. J. Park (2006). "An assessment of the tracer-  
 663 based approach to quantifying groundwater contributions to streamflow." *Water Resour.  
 664 Res.* **42**, 10.1029/2005wr004130  
 665 Jones, J. P., E. A. Sudicky and R. G. McLaren (2008). "Application of a fully-integrated surface-  
 666 subsurface flow model at the watershed-scale: A case study." *Water Resources Research*  
 667 **44**(3): W03407, 10.1029/2006wr005603  
 668 Justice, C. O., J. R. G. Townshend, E. F. Vermote, E. Masuoka, R. E. Wolfe, N. Saleous, D. P.  
 669 Roy and J. T. Morisette (2002). "An overview of modis land data processing and product  
 670 status." *Remote Sensing of Environment* **83**(1, 2): 3-15,  
 671 [http://dx.doi.org/10.1016/S0034-4257\(02\)00084-6](http://dx.doi.org/10.1016/S0034-4257(02)00084-6)  
 672 | [Kirkby, M. \(1988\). "Hillslope runoff processes and models." \*Journal of Hydrology\* \*\*100\*\*\(1, 3\):  
 673 315-339, \[http://dx.doi.org/10.1016/0022-1694\\(88\\)90190-4\]\(http://dx.doi.org/10.1016/0022-1694\(88\)90190-4\)](#)

674 [Kollet, S. J. \(2009\). "Influence of soil heterogeneity on evapotranspiration under shallow water](#)  
 675 [table conditions: Transient, stochastic simulations." Environmental Research Letters 4\(3\):](#)  
 676 [9.](#)  
 677 Kollet, S. J., I. Cvijanovic, D. Schüttemeyer, R. M. Maxwell, A. F. Moene and B. P. (2009).  
 678 "The influence of rain sensible heat, subsurface heat convection and the lower  
 679 temperature boundary condition on the energy balance at the land surface." *Vadose Zone*  
 680 *Journal* **8**(4): 12,  
 681 Kollet, S. J. and R. M. Maxwell (2006). "Integrated surface-groundwater flow modeling: A free-  
 682 surface overland flow boundary condition in a parallel groundwater flow model."  
 683 *Advances in Water Resources* **29**(7): 945-958,  
 684 Kollet, S. J. and R. M. Maxwell (2008). "Capturing the influence of groundwater dynamics on  
 685 land surface processes using an integrated, distributed watershed model." *Water*  
 686 *Resources Research* **44**(W02402): 18, doi:10.1029/2007WR006004  
 687 Kollet, S. J., R. M. Maxwell, C. S. Woodward, S. Smith, J. Vanderborght, H. Vereecken and C.  
 688 Simmer (2010). "Proof of concept of regional scale hydrologic simulations at hydrologic  
 689 resolution utilizing massively parallel computer resources." *Water Resources Research*  
 690 **46**(W04201): -, Doi 10.1029/2009wr008730  
 691 [Krakauer, N. Y., H. Li and Y. Fan \(2014\). "Groundwater flow across spatial scales: Importance](#)  
 692 [for climate modeling." Environmental Research Letters 9\(3\): 034003.](#)  
 693 Kumar, M., C. J. Duffy and K. M. Salvage (2009). "A second order accurate, finite volume  
 694 based, integrated hydrologic modeling (film) framework for simulation of surface and  
 695 subsurface flow." *Vadose Zone Journal*,  
 696 Maurer, E. P., A. W. Wood, J. C. Adam, D. P. Lettenmaier and B. Nijssen (2002). "A long-term  
 697 hydrologically based dataset of land surface fluxes and states for the conterminous united  
 698 states\*." *Journal of Climate* **15**(22): 3237-3251, 10.1175/1520-  
 699 0442(2002)015<3237:althbd>2.0.co;2  
 700 Maxwell, R. M. (2013). "A terrain-following grid transform and preconditioner for parallel,  
 701 large-scale, integrated hydrologic modeling." *Advances in Water Resources* **53**: 109-117,  
 702 <http://dx.doi.org/10.1016/j.advwatres.2012.10.001>  
 703 Maxwell, R. M., F. K. Chow and S. J. Kollet (2007). "The groundwater-land-surface-atmosphere  
 704 connection: Soil moisture effects on the atmospheric boundary layer in fully-coupled  
 705 simulations." *Advances in Water Resources* **30**(12): 2447-2466, Doi  
 706 10.1016/J.Advwatres.2007.05.018  
 707 Maxwell, R. M. and S. J. Kollet (2008). "Interdependence of groundwater dynamics and land-  
 708 energy feedbacks under climate change." *Nature Geosci* **1**(10): 665-669,  
 709 Maxwell, R. M. and S. J. Kollet (2008). "Quantifying the effects of three-dimensional subsurface  
 710 heterogeneity on hortonian runoff processes using a coupled numerical, stochastic  
 711 approach." *Advances in Water Resources* **31**(5): 807-817,  
 712 [Maxwell, R. M., J. D. Lundquist, J. D. Mirocha, S. G. Smith, C. S. Woodward and A. F. B.](#)  
 713 [Tompson \(2011\). "Development of a coupled groundwater-atmospheric model." Monthly](#)  
 714 [Weather Review doi: 10.1175/2010MWR3392\(139\): 96-116,](#)  
 715 Maxwell, R. M., M. Putti, S. Meyerhoff, J.-O. Delfs, I. M. Ferguson, V. Ivanov, J. Kim, O.  
 716 Kolditz, S. J. Kollet, M. Kumar, S. Lopez, J. Niu, C. Paniconi, Y.-J. Park, M. S.  
 717 Phanikumar, C. Shen, E. A. Sudicky and M. Sulis (2014). "Surface-subsurface model  
 718 intercomparison: A first set of benchmark results to diagnose integrated hydrology and  
 719 feedbacks." *Water Resources Research* **50**(2): 1531-1549, 10.1002/2013wr013725

Reed Maxwell 2/2/2015 5:06 AM  
 Moved (insertion) [1]

Miguez-Macho, G., Y. Fan, C. P. Weaver, R. Walko and A. Robock (2007). "Incorporating water table dynamics in climate modeling: 2. Formulation, validation, and soil moisture simulation." *Journal of Geophysical Research-Atmospheres* **112**(D13): -,  
 Mikkelsen, K. M., R. M. Maxwell, I. Ferguson, J. D. Stednick, J. E. McCray and J. O. Sharp (2013). "Mountain pine beetle infestation impacts: Modeling water and energy budgets at the hill-slope scale." *Ecohydrology* **6**(1): 64-72, 10.1002/eco.278  
 Osei-Kuffuor, D., R. M. Maxwell and C. S. Woodward "Improved numerical solvers for implicit coupling of subsurface and overland flow." *Advances in Water Resources*(0), <http://dx.doi.org/10.1016/j.advwatres.2014.09.006>  
 Osei-Kuffuor, D., R. M. Maxwell and C. S. Woodward (2014). "Improved numerical solvers for implicit coupling of subsurface and overland flow." *Advances in Water Resources* **74**(0): 185-195, <http://dx.doi.org/10.1016/j.advwatres.2014.09.006>  
 Qu, Y. and C. J. Duffy (2007). "A semidiscrete finite volume formulation for multiprocess watershed simulation." *Water Resources Research* **43**(W08419): 18, doi:10.1029/2006WR005752  
 Richards, L. A. (1931). "Capillary conduction of liquids in porous mediums." *Physics* **1**: 318-333,  
 Rihani, J. F., R. M. Maxwell and F. K. Chow (2010). "Coupling groundwater and land surface processes: Idealized simulations to identify effects of terrain and subsurface heterogeneity on land surface energy fluxes." *Water Resour. Res.* **46**: 1-14, doi:10.1029/2010WR009111  
 Rodell, M., I. Velicogna and J. S. Famiglietti (2009). "Satellite-based estimates of groundwater depletion in india." *Nature* **460**(7258): 999-1002,  
 Rodriguez-Iturbe, I. and A. Rinaldo (2001). *Fractal river basins: Chance and self-organization*, Cambridge University Press.  
 Schaap, M. G. and F. J. Leij (1998). "Database-related accuracy and uncertainty of pedotransfer functions." *Soil Science* **163**(10): 765-779,  
 Shi, Y., K. J. Davis, C. J. Duffy and X. Yu (2013). "Development of a coupled land surface hydrologic model and evaluation at a critical zone observatory." *Journal of Hydrometeorology* **14**(5): 1401-1420, 10.1175/jhm-d-12-0145.1  
 Sudicky, E., J. Jones, Y.-J. Park, A. Brookfield and D. Colautti (2008). "Simulating complex flow and transport dynamics in an integrated surface-subsurface modeling framework." *Geosciences Journal* **12**(2): 107-122, 10.1007/s12303-008-0013-x  
 Sulis, M., C. Paniconi, M. Marrocu, D. Huard and D. Chaumont (2012). "Hydrologic response to multimodel climate output using a physically based model of groundwater/surface water interactions." *Water Resources Research* **48**(12): W12510, 10.1029/2012wr012304  
 Taylor, R. G., B. Scanlon, P. Doll, M. Rodell, R. van Beek, Y. Wada, L. Longuevergne, M. Leblanc, J. S. Famiglietti, M. Edmunds, L. Konikow, T. R. Green, J. Chen, M. Taniguchi, M. F. P. Bierkens, A. MacDonald, Y. Fan, R. M. Maxwell, Y. Yechieli, J. J. Gurdak, D. M. Allen, M. Shamsudduha, K. Hiscock, P. J. F. Yeh, I. Holman and H. Treidel (2013). "Ground water and climate change." *Nature Clim. Change* **3**(4): 322-329,  
 Therrien, R., E. Sudicky, Y. Park and R. McLaren (2012). *Hydrogeosphere: A three-dimensional numerical modelling describing fully-integrated subsurface and surface flow and transport. User guide*. Waterloo, Ontario, Canada, Aquanty Inc.

Reed Maxwell 2/2/2015 5:06 AM

**Deleted:** Nir, Y. K., L. Haibin and F. Ying

Reed Maxwell 2/2/2015 5:06 AM

**Moved up [1]:** (2014). "Groundwater flow across spatial scales: Importance for climate modeling." *Environmental Research Letters* **9**(3): 034003, -



770 van Genuchten, M. T. (1980). "A closed-form equation for predicting the hydraulic conductivity  
 771 of unsaturated soils." Soil Science Society of America Journal **44**(5): 892-898,  
 772 VanderKwaak, J. E. and K. Loague (2001). "Hydrologic-response simulations for the r-5  
 773 catchment with a comprehensive physics-based model." Water Resources Research  
 774 **37**(4): 999-1013,  
 775 Williams, J. L. and R. M. Maxwell (2011). "Propagating subsurface uncertainty to the  
 776 atmosphere using fully-coupled, stochastic simulations." Journal of Hydrometeorology,  
 777 doi:10.1175/2011JHM1363.1  
 778 Wood, B. D. (2009). "The role of scaling laws in upscaling." Advances in Water Resources  
 779 **32**(5): 723-736, <http://dx.doi.org/10.1016/j.advwatres.2008.08.015>  
 780 Wood, E. F., J. K. Roundy, T. J. Troy, L. P. H. van Beek, M. F. P. Bierkens, E. Blyth, A. de Roo,  
 781 P. Döll, M. Ek, J. Famiglietti, D. Gochis, N. van de Giesen, P. Houser, P. R. Jaffé, S.  
 782 Kollet, B. Lehner, D. P. Lettenmaier, C. Peters-Lidard, M. Sivapalan, J. Sheffield, A.  
 783 Wade and P. Whitehead (2011). "Hyperresolution global land surface modeling: Meeting  
 784 a grand challenge for monitoring earth's terrestrial water." Water Resources Research  
 785 **47**(5): W05301, 10.1029/2010wr010090  
 786 Xia, Y., K. Mitchell, M. Ek, B. Cosgrove, J. Sheffield, L. Luo, C. Alonge, H. Wei, J. Meng, B.  
 787 Livneh, Q. Duan and D. Lohmann (2012). "Continental-scale water and energy flux  
 788 analysis and validation for north american land data assimilation system project phase 2  
 789 (nldas-2): 2. Validation of model-simulated streamflow." Journal of Geophysical  
 790 Research: Atmospheres **117**(D3): D03110, 10.1029/2011jd016051  
 791  
 792